Amplitude-aware permutation entropy: Illustration in spike detection and signal segmentation

Amplitude-aware Permutation Entropy: Illustration in Spike Detection and Signal Segmentation

Hamed Azami[1] and Javier Escudero[2]

[1,2]*Institute for Digital Communications, School of Engineering, University of Edinburgh,*
Edinburgh, King's Buildings, EH9 3JL, UK
Emails:[1]hamed.azami@ed.ac.uk; [2]javier.escudero@ed.ac.uk

Abstract:

Background and Objective: Signal segmentation and spike detection are two important biomedical signal processing applications. Often, non-stationary signals must be segmented into piece-wise stationary epochs or spikes need to be found among a background of noise before being further analyzed. Permutation entropy (PE) has been proposed to evaluate the irregularity of a time series. PE is conceptually simple, structurally robust to artifacts, and computationally fast. It has been extensively used in many applications, but it has two key shortcomings. First, when a signal is symbolized using the Bandt-Pompe procedure, only the order of the amplitude values are considered and information regarding the amplitudes is discarded. Second, in the PE, the effect of equal amplitude values in each embedded vector is not addressed. To address these issues, we propose a new entropy measure based on PE: the amplitude-aware permutation entropy (AAPE).

Methods: AAPE is sensitive to the changes in the amplitude, in addition to the frequency, of the signals thanks to it being more flexible than the classical PE in the quantification of the signal motifs. To demonstrate how the AAPE method can enhance the quality of the signal segmentation and spike detection, a set of synthetic and realistic synthetic neuronal signals,

1

electroencephalograms and neuronal data are processed. We compare the performance of AAPE in these problems against state-of-the-art approaches and evaluate the significance of the differences with a repeated ANOVA with post-hoc Tukey's test.

Results: In signal segmentation, the accuracy of AAPE-based method is higher than conventional segmentation methods. AAPE also leads to more robust results in the presence of noise. The spike detection results show that AAPE can detect spikes well, even when presented with single-sample spikes, unlike PE. For multi-sample spikes, the changes in AAPE are larger than in PE.

Conclusion: We introduce a new entropy metric, AAPE, that enables us to consider amplitude information in the formulation of PE. The AAPE algorithm can be used in almost every irregularity-based application in various signal and image processing fields. We also made freely available the Matlab code of the AAPE.

Keywords: Signal irregularity, amplitude-aware permutation entropy, spike detection, signal segmentation, electroencephalogram, extracellular neuronal data.

1. Introduction

Quantifiers based on information theory concepts, such as different entropy approaches and statistical complexities, can be used to characterize the dynamics associated with time series [1]. Entropy, which is a popular and powerful indicator of the regularity of signals, has been extensively used in various signal and image processing applications [2-5]. The level of uncertainty and irregularity of the signal or system can be measured with entropy concepts. Higher entropy values generally demonstrate higher uncertainty, while lower entropy ones illustrate more regularity and certainty of a time-series [6].

Several entropy methods, such as approximate entropy (ApEn) [7], sample entropy (SaEn) [8], fuzzy entropy (FuEn) [9], permutation entropy (PE) [10] and wavelet entropy [11], have been introduced over the few past decades to measure the irregularity of time series. Each of them has its own advantages and disadvantages [12, 13].

PE is based on the permutation patterns or the order relations among values of a signal [14]. In fact, PE was naturally proposed based on comparing the order of neighboring relative values, rather than by apportioning amplitudes according to different levels [14]. Compared with other entropy approaches, PE is theoretically simple, relatively robust to observational and dynamical noise, and computationally fast. Moreover, PE is more robust than the zero-crossing rate to the signal length, although both have relatively similar theoretically notions [10]. These characteristics make the PE an appealing tool used in a large number of real world signal and image processing applications [14-16]. PE-based approaches have been used in various studies, such as distinguishing noise from chaos [17], dependences between time series [18], and econophysics [19] and physiological applications [20-22]. PE has been widely used in biomedical signal processing study, such as epilepsy [23], anesthesiology [24], and cognitive neuroscience [25] using electroencephalogram (EEG) and electrocardiogram (ECG) time series.

In spite of the aforementioned advantages over other feature extraction algorithms, PE has two main shortcomings. First, the mean value of amplitudes and the differences between neighboring samples are not considered while a signal is symbolized by the original PE definition. As a result, vectors with very dissimilar amplitudes may be mapped to the same symbol. Second, the problem arising when two samples have equal amplitude values (which is particularly relevant for digitized time series) was not precisely solved in the basic definition of PE [14].

In [26], a modified algorithm was proposed to address the first abovementioned PE's limitation, i.e., its inability to differentiate between distinct patterns of a certain motif. Their approach stands for the fact that patterns might be too disparate in amplitudes and variances. It weights the relative frequency of each extracted vector (associated with every motif) with the variance of the corresponding part of the signal [26]. This leads to a powerful and widely applicable tool. However, this technique would not be able to distinguish the case where a constant value is added to the original signal because its variance would not change. In addition, it does not allow to customize how much importance is given to the amplitude information represented by the variance value.

Bian *et al.* tackled the equal values' problem [27]. They used the same symbols to represent equal values. As a result, the algorithm yields a more accurate characterization of system states. In spite of its advantage for long signals, the number of potential motifs increases considerably in comparison with the original PE, which might yield the modified algorithm unreliable in the case of short signals. They employed three groups of heart rate variability data to show the performance of their method [27]. In [28], an algorithm based on Lyapunov exponent was also proposed to overcome the equal values' problem. Although it improves the performance of PE, this algorithm is sensitive to the precision regulation factor α.

In order to overcome the PE drawbacks and improve on existing alternatives, in this paper, we propose two novel modifications of PE, leading to an amplitude-aware PE (AAPE). We also illustrate them using synthetic and real signals for signal segmentation and spike detection applications.

The EEG is a signal that reflects the electrical activity of a large group of neurons of the brain. It is a powerful measure to diagnose and treat the brain diseases, disorders, and abnormalities [6, 29]. It is frequently needed to label the EEG signals by segments of similar statistical characteristics that are meaningful to clinicians and neurophysiologists [29]. Within each segment, the signals are considered statistically stationary, usually with similar mean and standard deviation [29, 30]. There are a number of approaches to segment time series based on nonlinear analysis [30-35]. To understand the performance of the proposed method for signal segmentation, two kinds of signals, namely, synthetic signals and real EEG data, are used.

Spike detection is a widely used kind of analysis applied to extracellular neuronal signals to understand brain diseases and abnormalities [1, 36]. The quality of a spike detection method remarkably influences the performance of subsequent steps, such as spike sorting (i.e., grouping the recorded spikes into clusters based on the similarity of their shapes). Errors in detecting the number and location of spikes will inevitably propagate through all later analyses [37, 38]. To understand the performance of the proposed method for spike detection, two kinds of signals, including realistic synthetic and real neuronal data, are utilized.

The paper is organized as follows. In Section 2, we explain the concept of PE. Next, the proposed modifications to PE are described in Section 3. In Section 4, the synthetic signals and real EEG data for signal segmentation and realistic synthetic and real neuronal data for spike detection are presented. Then, the results of the proposed method and the conventional ones are compared and discussed in Section 5. Finally, Section 6 provides the conclusion of the paper.

2. Permutation Entropy

5

Assume we have a given time series of length N, and let the time series be $\mathbf{y} = \{y_1, y_2, ..., y_N\}$. For each time t, we embed the signal $\mathbf{y}$ in a d-dimensional space to obtain the reconstruction vectors $Y_t^{d,l} = \{y_t, y_{t+l}, ..., y_{t+(d-2)l}, y_{t+(d-1)l}\}$ for $t=1,2,...,N-(d-1)l$, where d and l denote the embedding dimension and the time delay, respectively. Next, each $Y_t^{d,l}$ is arranged in an increasing order, with integer indices from 0 to $d-1$, as $\{y_{t+(j_1-1)l}, y_{t+(j_2-1)l}, ..., y_{t+(j_{d-1}-1)l}, y_{t+(j_d-1)l}\}$, where j_* is the (time) index of the element in the reconstruction vector. For different samples, there are $d!$ potential ordinal patterns or $d!$ symbol sequences π, termed "motifs" [10]. Then we can count the occurrences of the order pattern i, which is denoted as $f(\pi_i)$, $i=1, 2,..., d!$. For each π_i, $p(\pi_i)$ represents the relative frequency as follows:

$$p(\pi_i) = \frac{f(\pi_i)}{N - d + 1} \tag{1}$$

Finally, the PE is computed as follows [10, 14]:

$$\text{PE}(\mathbf{y}, d, l) = -\sum_{\pi_i=1}^{\pi_i=d!} p(\pi_i) \ln p(\pi_i) \tag{2}$$

When all motifs have equal probability, the largest value of PE is obtained, which has a value of $\ln(d!)$. In contrast, if there is only one $p(\pi_i)$ different from zero, which illustrates a completely regular signal, the smallest value of PE is obtained [10, 14].

Due to the key role of the embedding dimension d in PE, an important issue is choosing the appropriate value for it. In order to work with reliable statistics when calculating PE, it is highly recommended $d! \ll N$ [1, 21]. In addition, when d is too large, the computation time will be higher. On the other hand, when d is high, the number of accessible states will be large, and the

value of the PE will probably be more reliable. All in all, we should make a trade-off between the aforementioned cases.

3. Amplitude-aware Permutation Entropy

The original PE has two main drawbacks:

1) Since PE solely considers the ordinal structure of a time-series, some crucial information might be missed. For example, {1,10,2} and {1,3,2} have similar permutations, leading to the same motif "021" because the extent of the differences between sequential samples are not considered in the original definition of PE. Another example is the fact that both {1,3,2} and {11,13,12} have the same ordinal pattern "021" because the mean value of these samples is not considered in the original PE method.

2) When there are equal values in the vector of values, Bandt and Pombe [10] proposed ranking the possible equalities based on their order of emergence or solving this condition by adding noise. Considering the first alternative, for instance, the permutation pattern for both {1,2,4} and {1,4,4} would be "012". As an another example, assume $z_1=\{1,2,2,2\}$ and $z_2=\{1,2,3,4\}$. The PE of z_1 is exactly the same as z_2, both equalling 0 although, unlike z_1, z_2 is strictly ascending. Adding noise may not lead to a precise answer because, for example, {1,4,4} has two possible permutation patterns as "012" and "021" and there are not any differences between them. It should be noted that this problem is particularly relevant for digitized signals.

To address the first problem, we suggest adding a variable contribution, depending on amplitude, instead of a constant number to each level in the histogram representing the probability of each motif. That is, in PE, when a vector is assigned to a motif, the histogram bin corresponding to the

motif is incremented by one. In contrast, in AAPE, a relative normalized probability

$\dfrac{A}{d}\displaystyle\sum_{k=1}^{d}\left|y_{t+(k-1)l}\right|+\dfrac{1-A}{d-1}\displaystyle\sum_{k=2}^{d}\left|y_{t+(k-1)l}-y_{t+(k-2)l}\right|$ is added to the corresponding motif. *A* is the adjusting

coefficient related to the mean value and difference between consecutive samples to make the

AAPE algorithm more flexible. *A* is in the range [0,1]. Finally, the amplitude-aware version of

Equation 1 is normalized by the total sum of the contributions. In brief, the pseudo code of the

AAPE algorithm is presented in Figure 1:

```
begin

  $p(\pi_i^{d,l}) = 0$ ;

  for $t=1$ to $N-d+1$ do

        for $i=1$ to $d!$ do

              if $\text{type}(Y_t^{d,l}) = \pi_i^{d,l}$ , then

                    $p(\pi_i^{d,l}) = p(\pi_i^{d,l}) + \left( \dfrac{A}{d} \displaystyle\sum_{k=1}^{d} \left| x_{t+(k-1)l} \right| + \dfrac{1-A}{d-1} \displaystyle\sum_{k=2}^{d} \left| x_{t+(k-1)l} - x_{t+(k-2)l} \right| \right)$ ;

                    end

        end

  end
```

$$p(\pi_i^{d,l}) = \frac{p(\pi_i^{d,l})}{\displaystyle\sum_{t=1}^{N-d+1} \left(\dfrac{A}{d} \displaystyle\sum_{k=1}^{d} \left| y_{t+(k-1)l} \right| + \dfrac{1-A}{d-1} \displaystyle\sum_{k=2}^{d} \left| y_{t+(k-1)l} - y_{t+(k-2)l} \right| \right)} ;$$

$$AAPE(d,l,n) = -\sum_{\pi_k=1}^{\pi_k=d!} p(\pi_k) \ln p(\pi_k) ;$$

```
end
```

Figure 1. The pseudo code of the AAPE algorithm to take into account the mean value of amplitudes and differences between amplitude values.

For the practical uses of AAPE, we, similarly to the proposers of PE [10], recommend to assume $l=1$, because $l>1$ may be similar to down-sampling without considering the frequency characteristics of the signals, something that might lead to aliasing. Furthermore, to consider

multiple temporal scales, the multiscale framework by Costa et al. [39] or its improved version proposed by Azami et al. [20] can be used. Here, we choose $l=1$ for signal segmentation application. For the spike detection application, assume we have a single-sample spike as {3,1,10,2,5}, the differences between two amplitude values with $l=2$ are larger than those with $l=1$. However, for multi-sample spikes, it is recommended to use a delay time larger than 1. Assuming a multi-sample spike as {1,3,10,4,2}, the AAPE with $l=2$ can detect the spike better than the AAPE with $l=1$. In fact, multi-sample spike detection application is an exception for the choice of the time delay l. In this piece of research, because there is no information to demonstrate the real neuronal signals consist of only multi-sample spikes, we choose $l=1$.

To select an appropriate value of A, since the importance of the mean value of amplitudes and the differences of the amplitude values are equal, it is recommended to choose $A=0.5$. Nevertheless, it is recommended to change the value of A in case we want to emphasize more on either the amplitude values change or average of amplitude values. For example, in spike detection, because the difference between two successive sample points is much more important than the mean value of amplitudes, it is recommended that $A \ll 0.5$. In contrast, in signal segmentation applications, the mean of amplitude values and the differences of successive sample points are equally important and, therefore, it is better to choose $A=0.5$.

For example, for signal segmentation application and for {1,3,2} and {11,13,12}, the contributions to the count of the motifs ("021" in both cases) are 1.75 and 6.75, respectively. Thus, unlike PE, AAPE can discriminate the change in the average. For spike detection and for {1,10,2} and {1,3,2}, assuming $A=0.02$, the corresponding contributions would respectively be 8.42 and 1.51 even though both motifs are "021". This makes the effect of motif "021" associated with {1,10,2} considerably larger when compared with the other potential motifs. Thus, using this procedure,

spikes may be detected more easily. It is worth noting that for this application, AAPE is not very sensitive to the values of *A*. For example, assuming *A*=0.1, 0.2, or even 0.5 leads to detect the spikes correctly.

The second drawback can be overcome by the following approach. To start with, all potential permutations of similar states are considered. Then, all possible contributions coming from motifs with a tie (i.e., same state) are divided by the number of potential permutations of those equal states. For example, assume {1,2,3,2,2} and *d*=2, leading to "01" (full contribution associated with {1,2}), "01" (full contribution associated with {2,3}), "10" (full contribution associated with {3,2}, "01" (associated with half the contribution of {2,2}), and "10" (associated with the other half of the contribution of {2,2}). In this case, the entropy value considering equal (i.e., half) contributions of the motif {2,2} is

$$AAPE(x,1,2) = -(2.5/4)\ln(2.5/4) - (1.5/4)\ln(1.5/4) = 0.6616$$. As an additional example, consider *d*=3, leading to "012" (full contribution associated with {1,2,3}), "201" (associated with half the contribution of {2,3,2}), "021" (associated with the other half of the contribution of {2,3,2}), "012" (associated with half the contribution of {3,2,2}), "021" (associated with the other half of the contribution of {3,2,2}). In this case, the entropy value considering equal (i.e., half) contributions of the motifs {2,3,2} and {3,2,2} are

$$AAPE(x,1,3) = -(1.5/3)\ln(1.5/3) - (1/3)\ln(1/3) - (0.5/3)\ln(0.5/3) = 1.0114$$. In this way, the proposed method can discriminate between the strictly ascending/descending and only ascending/descending sequences. It is worth noting that the combination of the first and second proposed algorithms makes to the proposed method.

4. Evaluation Signals

For evaluation of the proposed method, two kinds of synthetic data for signal segmentation and spike detection, and real neuronal and EEG data are used. The existing and proposed approaches were implemented using MATLAB R2010a from Math Works, Inc.

4.1. Synthetic Signals

4.1.1. Signal Segmentation Application

In this paper, a dataset including 40 synthetic multi-component signals was used. In order to make signals similar to actual recordings, we added white Gaussian noise (WGN) to synthetic signals. The WGN has a normal distribution with zero mean and unit variance. The equation of each of multi-component signals is as follows:

$$y(t) = x(t) + n(t) \tag{3}$$

where $n(t)$ denotes WGN with different signal-to-noise ratios (SNRs) and $x(t)$ is produced by concatenating seven multi-component epochs. One signal of the synthetic multi-component database, consisting of even epochs with random duration between 5.5 to 8 s (named test signal), is as follows:

Epoch 1: $0.5\cos(\pi t)+1.5\cos(4\pi t)+4\cos(5\pi t)$,

Epoch 2: $0.7\cos(\pi t)+2.1\cos(4\pi t)+5.6\cos(5\pi t)$,

Epoch 3: $1.5\cos(2\pi t)+4\cos(8\pi t)$,

Epoch 4: $1.5\cos(\pi t)+4\cos(4\pi t)$,

Epoch 5: $0.5\cos(\pi t)+1.5\cos(2\pi t)+ 0.8\cos(3\pi t)+3.5\cos(5\pi t)$,

Epoch 6: 4.5cos(3πt)+2.2cos(5πt),

Epoch 7: 0.8cos(πt)+cos(3πt)+3cos(5πt).

We utilize $n(t)$ with SNR=5, 10, and 15 dBs. Note that the test signal is a general and comprehensive time series since Epochs 1 and 2 are different almost only in terms of amplitude, Epochs 3 and 4 are different nearly only in terms of frequency, and the other adjacent epochs have the different amplitude and frequency characteristics at the same time. In addition, each epoch has different random time duration. All in all, we have all possible states in only one signal).

4.1.2. Spike Detection Application

Because of the lack of ground-truth data (i.e., spike timings for each neuron), spike detection approaches are frequently demanding to evaluate. In [40], the generation and transmission of intracellular signals from neurons to an extracellular electrode were modeled and a set of MATLAB functions based on this were provided. The codes were used here to generate a set of realistic synthetic neural signals. They produce realistic neuronal signals from a set of nearby neurons including interference from more distant neurons and Gaussian noise. These data best resemble the output of deep mesio-temporal brain discharges observed at cortical electrodes. The model also includes correlated and uncorrelated spike noises in neuronal data as well as some Gaussian noise, to imitate the effect of thermal and amplifier noise [40]. By following this synthesizing method, we have randomly generated 40 realistic synthetic neuronal data each including Gaussian noise with SNR=20 dB. Each signal contains 12 to 14 spikes.

4.2. Real Signals

4.2.1. Signal Segmentation Application

In the second step, we employed real EEG signals for signal segmentation. As mentioned earlier, the registration of electrical activity of the neurons in the brain, EEG, is a significant tool to identify and treat some neurological disorders like epilepsy. In this paper, several EEG signals recorded from the scalp of a number of patients are used. The length of signals and the sampling frequency respectively are 30 seconds and 256 Hz. The data were prepared in the Signal Processing Research Centre at Queensland University of Technology, Queensland, Australia. The data are used in many signal segmentation approaches [30, 31, 41] provided by Prof. Hamid Hassanpour from the Department of Information Technology and Computer Engineering, Shahrood University of Technology, Iran.

4.2.2. Spike Detection Application

In addition to a set of realistic synthetic neural data, we assessed the proposed and conventional approaches for the real neuronal signal. The data is a part of a publicly available real signal of the CARMEN project managed by Prof. Leslie S. Smith (http://www.carmen.org.uk/). It is around 900 s long sampled at 20,000 Hz.

5. Results and Discussion

In this section, the behaviors of PE and AAPE using synthetic signals and real EEG data for signal segmentation and realistic synthetic and real neuronal signals for spike detection are assessed.

5.1. Synthetic signals

5.1.1. Signal Segmentation Application

For signal segmentation, the PE/AAPE values of the signal are computed using the sliding window with the length w moving along the signal. Variation in the PE or AAPE is used to obtain the segment boundaries as follows:

$$G_m = \left| PE_{m+1} - PE_m \right| \qquad m = 1, 2, ..., n\text{-}1 \qquad\qquad (4)$$

where m and n stand for the number of analyzed windows and the total number of analyzed windows, respectively. Note that $n = \left\lfloor \dfrac{N-w}{OL \times w} \right\rfloor$, where N and OL are the length of the signal and the percentage of overlapping of the sliding window, respectively. For window-based signal segmentation and spike detection approaches, two parameters, including the length of the window and percentage of overlapping of the sliding window, should be chosen by trial and error [30, 35, 36, 38, 42]. In this paper, the mean value of $G = \{G_1, G_2, ..., G_{n-1}\}$ is defined as threshold. When the local maximum is larger than the defined threshold, the current sample is chosen as the boundary of segment.

The test signal introduced in subsection 4.1.1. is shown in Figure 2(a). Figures 2(b) and 2(c) respectively show the AAPE of the signal and changes in the G function. As it can be seen in Figure 2, all six boundaries are correctly detected. The signal in Figure 2(a) is also segmented using PE. Its result is depicted in Figure 3(c). Two boundaries are not detected by PE (missed boundaries) as well as one boundary is incorrectly detected (false boundary). It should be added that for each signal used here, using PE and AAPE, all employed parameters are alike. As mentioned earlier, because the differences between sample points for signal segmentation are relatively as important as their average, we choose $A=0.5$, even though changing these values will not change the results significantly. The window length and percentage of overlapping are chosen

as much as 50 samples (2.5 s) and 50%, respectively. Considering the length of the signal and $3! \ll 50$, the embedding dimension is chosen as 3. These parameters are used for all synthetic signals for segmentation application.

For both the signal segmentation and spike detection applications, two different metrics, including true positive per signal (TPS) and false positive per signal (FPS) ratios are used to evaluate the performance of the proposed and conventional methods. These parameters are defined as $TPS = \left(NS_t \big/ NS \right)$ and $FPS = \left(NS_f \big/ NS \right)$; where NS_t and NS_f indicate the number of true and falsely detected boundaries for each signal, respectively. NS denotes the actual number of signal segments' boundaries or spikes for each signal.
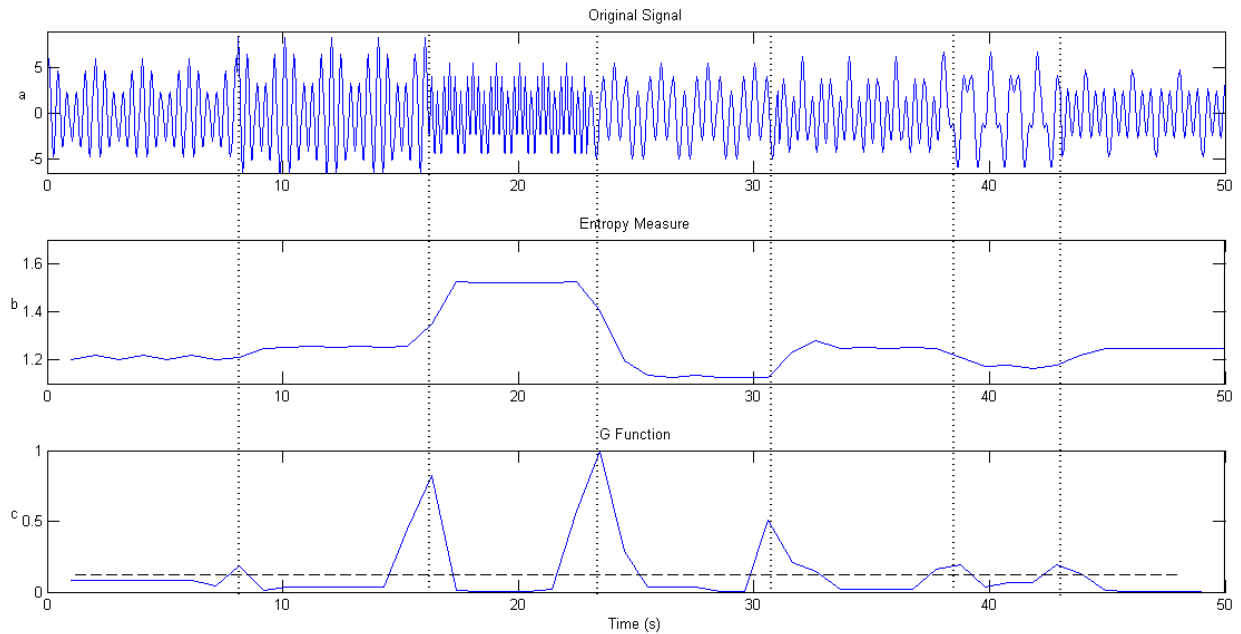

16

Figure 2. Result of the proposed method for the synthetic signal. (a) Original signal, (b) extracted features using the AAPE, and (c) *G* function result. The boundaries for all seven segments are accurately detected.
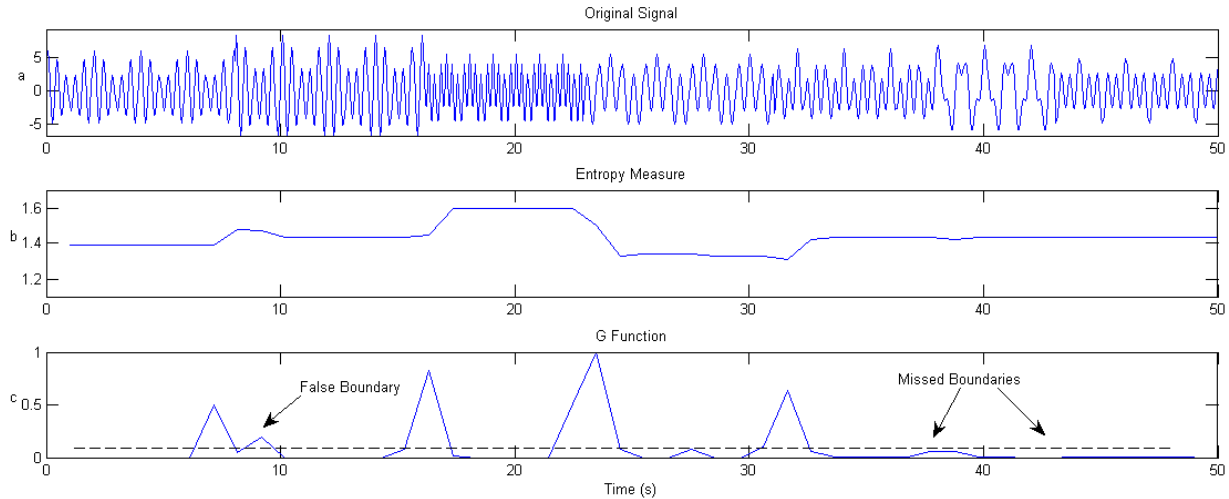

Figure 3. Results obtained by the PE method for the synthetic signal. (a) Original signal, (b) extracted features using the PE, and (c) *G* function result.

To compare the proposed method with the state-of-the-art signal segmentation methods that usually have a pre-processing step, we use a discrete wavelet transform (DWT). In Table 1, the results of the segmentation for 40 synthetic signals using AAPE with DWT, PE with DWT, the method based on DWT, Katz's fractal dimension (KFD), and bee colony optimization (BCO) [41], the approach based on DWT, KFD, and particle swarm optimization (PSO), AAPE, PE, GLR and WGLR are shown. Note that the key difference between the method proposed in [41] and [35] is the cost functions used in these papers as well as BCO usually leads to a better performance in comparison with PSO. The DWT used for synthetic signals is with Daubechies wavelet of order 8. The parameters of PSO are: population size = 30, $C_1 = C_2 = 2$, dimension=2, and iteration = 50

according to [35]. The parameters of BCO are defined as: population size = 30, dimension = 2, and iteration = 50 according to [41].

Among the existing and proposed methods, the best algorithm in terms of TPS average is AAPE with DWT. Moreover, the SD values demonstrate that the proposed method is the most stable method. Moreover, the results show for lower SNRs, the SD values usually increase, as expected. The reason why AAPE works better than FD-based approaches is that the KFD may be slightly unreliable when the length of the signal is small [43]. In terms of FPS, AAPE and DWT, the approach based on DWT, KFD, and BCO, and the method using WT, KFD, and PSO are relatively similar. Although in terms of TPS, GLR and WGLR methods have relatively better performance for all SNRs, when considering FPS, both PE-based signal segmentation approaches are far superior to the GLR and WGLR methods. Moreover, considering SNRs, PE and AAPE are more robust than GLR and WGLR. As expected theoretically, AAPE, in comparison with PE, has better performance in terms of FPS and TPS. Comparing the results obtained by the method using AAPE/PE and DWT with AAPE/PE method without DWT shows a pre-processing step can improve the performance of a method considerably.

A repeated measures analysis of variance (ANOVA) was employed to explore the differences among the means of the TPS and FPS values obtained by the proposed and existing methods. When the corresponding p-value was lower than 0.05, thus indicating a significant effect of the choice of method, the Tukey's range test was used to find whether the results obtained with the proposed method were significantly different from those obtained by each of the existing approaches. According to the repeated ANVOA and Tukey's range test, the proposed signal segmentation

18

method is significantly better than the conventional methods in terms of TPS using synthetic signals.

Table 1. Signal segmentation results of the aforementioned improved and existing methods using the multi-component synthetic data.

Signal Segmentation based on DWT and AAPE			
SNR	5 dB	10 dB	15 dB
TPS (mean ± SD)	0.93 ± 0.11	0.94 ± 0.10	0.95 ± 0.09
FPS (mean ± SD)	0.11 ± 0.14	0.09 ± 0.13	0.05 ± 0.09
Signal Segmentation based on DWT and PE			
SNR	5 dB	10 dB	15 dB
TPS (mean ± SD)	0.89 ± 0.12	0.91 ± 0.11	0.92 ± 0.10
FPS (mean ± SD)	0.18 ± 0.15	0.16 ± 0.13	0.10 ± 0.13
Signal Segmentation based on DWT, KFD, and BCO [41]			
SNR	5 dB	10 dB	15 dB
TPS (mean ± SD)	0.83 ± 0.14	0.90 ± 0.15	0.94 ± 0.13
FPS (mean ± SD)	0.11 ± 0.15	0.06 ± 0.13	0.04 ± 0.09
Signal Segmentation based on WT, KFD, and PSO [35]			
SNR	5 dB	10 dB	15 dB
TPS (mean ± SD)	0.81 ± 0.14	0.87 ± 0.15	0.93 ± 0.12
FPS (mean ± SD)	0.27 ± 0.16	0.17 ± 0.15	0.05 ± 0.13
AAPE-based Method			
SNR	5 dB	10 dB	15 dB
TPS (mean ± SD)	0.90 ± 0.15	0.90 ± 0.15	0.94 ± 0.14
FPS (mean ± SD)	0.71 ± 0.20	0.61 ± 0.18	0.49 ± 0.16
PE-based Method			
SNR	5 dB	10 dB	15 dB
TPS (mean ± SD)	0.85 ± 0.16	0.86 ± 0.14	0.87 ± 0.14
FPS (mean ± SD)	0.78 ± 0.21	0.72 ± 0.19	0.60 ± 0.18
WGLR Method [44]			
SNR	5 dB	10 dB	15 dB
TPS (mean ± SD)	0.91 ± 0.15	0.93 ± 0.13	0.95 ± 0.13
FPS (mean ± SD)	2.3 ± 0.51	1.6 ± 0.49	1.2 ± 0.42
GLR Method			
SNR	5 dB	10 dB	15 dB
TPS (mean ± SD)	0.81 ± 0.15	0.87 ± 0.15	0.93 ± 0.13
FPS (mean ± SD)	2.8 ± 0.95	2.1 ± 0.73	1.6 ± 0.54

5.1.2. Spike Detection Application

We divide spikes into two main groups: single-sample and multi-sample spikes. Single-sample spike means that the spike has only one sample point much higher than its neighboring sample points, whereas in multi-sample spikes, the amplitude increases/decreases and then decreases /increases gradually, i.e., this kind of spikes includes more than one sample point.

In order to understand the performance of PE and AAPE, 40 synthetic impulse signals with 1000 sample points, with added white Gaussian noise with SNR=20 dB, are used. The obtained results using PE and AAPE are shown in Figure 4. Each error bar depicts the SD of the average of results of 40 signals for each of synthetic data. Since there is not any trend in single-sample spike, the PE cannot detect the spike. However, AAPE is able to detect the spike, because it takes into account the effect of the amplitude. This fact is depicted in Figure 4.

We also assess the capability of AAPE, in comparison with PE, to detect multi-sample spikes. As mentioned in the subsection 4.1.2, we use 40 realistic synthetic signals. One of 40 signals, which is randomly selected, includes 13 spikes and is depicted in Figure 5.

As can be seen in Figure 5, both the PE and AAPE can detect this kind of spikes, even though the differences of the results of AAPE is larger than PE. For multi-sample spikes, because there is a descending/ascending inclination at first step and an ascending/descending slope in the second step, both approaches can follow this trend. Inasmuch as for spike detection, the differences between sample points are much more important than their average, we choose $A = 0.02$, although changing this value will not change the results considerably. In addition, considering the length of the window, the embedding dimension was 4. Note that we have evaluated the results with different delay time values and l=1 was better than the other ones.

We evaluate the performance of the proposed and existing methods using 40 realistic synthetic neuronal data proposed in [40]. These results are shown in Table 2. The reason why we use singular spectrum analysis (SSA) as a filter is that SSA was the best algorithm in comparison with DWT, Kalman filter, and Savitzky-Golay filter for neuronal signals [38]. We compare the proposed method using SSA with the spike detection based on FD and SSA as the best algorithm in [38] and normalized cumulative energy difference (NCED) as the best method proposed in [45]. NCED was inspired by the fact that the energy in a spike (either positive or negative) should be greater than the energy in noise of the same length [45]. The results show that in terms of TPS, the proposed method based on AAPE with and without SSA, and the method based on KFD and SSA are the best algorithms. In terms of FPS, the approach based on KFD and SSA is slightly better than the proposed method using AAPE and SSA. The reason why the KFD is better here is that the window moving along the signal has an acceptable length (400) [43]. Although SSA does not improve the TPS ratios of AAPE- and PE-based spike detection, the FPS ratios considerably decrease by using SSA. Note that the SSA used here and [38] has a window length equal to 20 sample points that was selected with trial and error.

The statistical tests show that, in terms of TPS and FPS, the proposed method based on AAPE with SSA and the method based on KFD and SSA, are the two best algorithms for the realistic synthetic neuronal data. Their performance was not significantly different, although we will show the proposed spike detection approach leads to a slightly higher TPS value using the real neuronal time series.
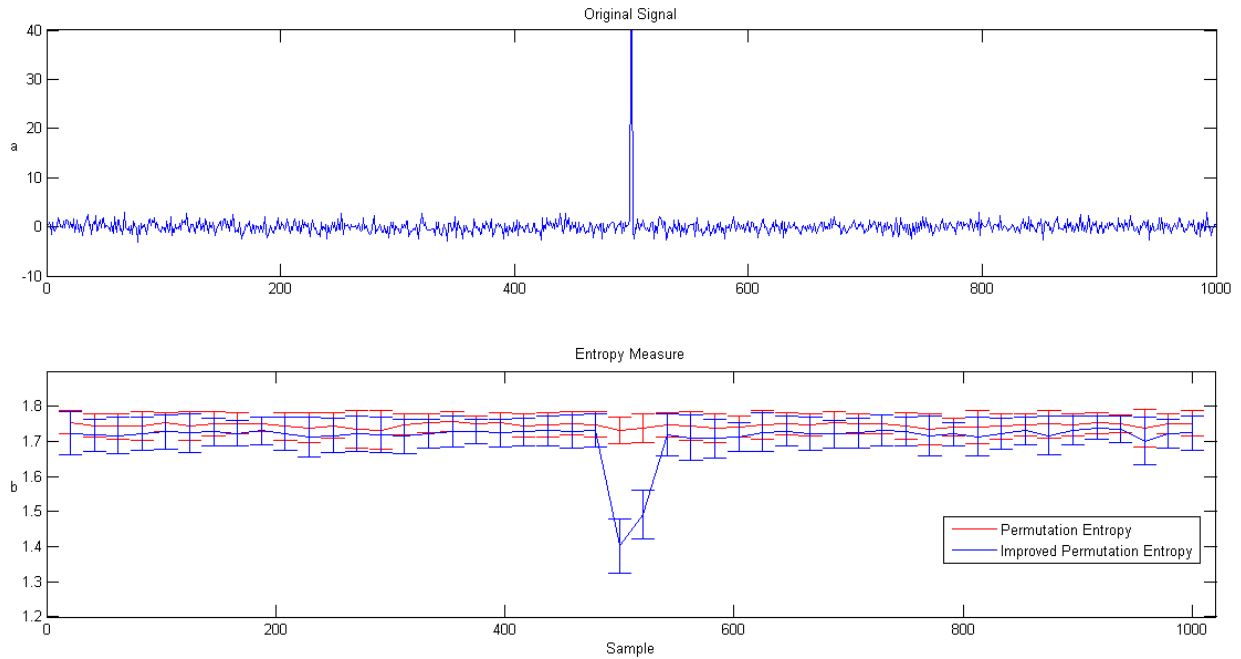
Figure 4. Mean value of results of the PE and AAPE computed from 40 different synthetic test signals for spike detection.
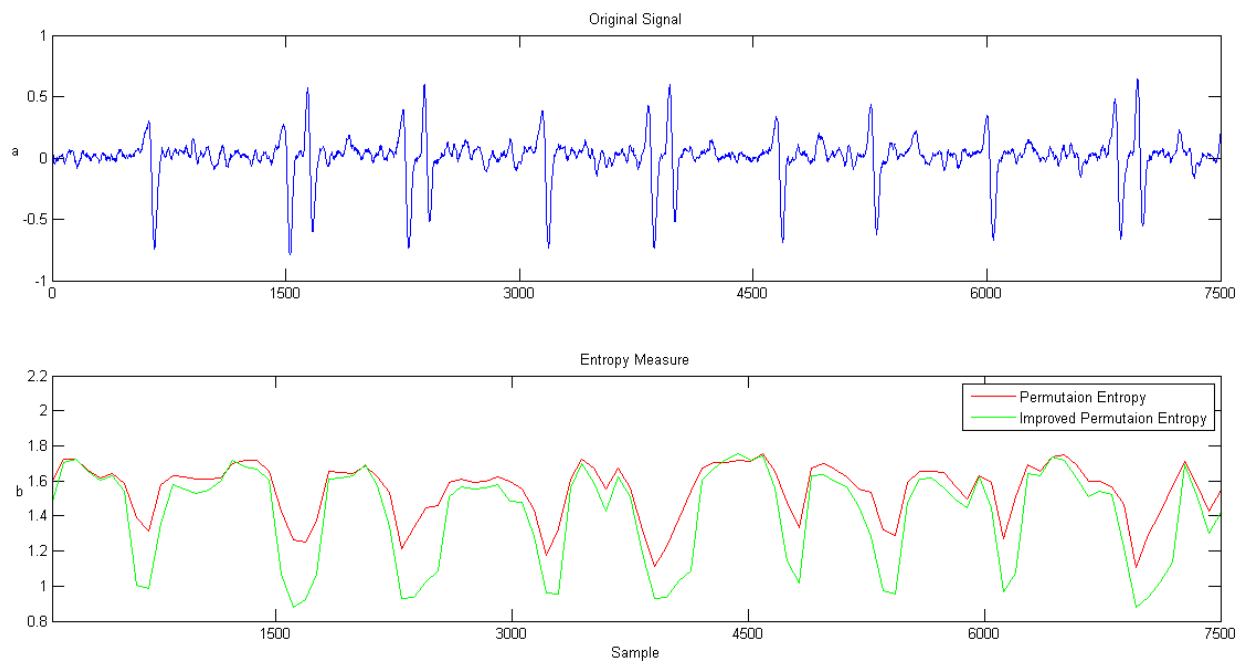
Figure 5. Results of the PE and AAPE using synthetic spike signal. (a) Original signal, (b) extracted features using PE and AAPE.

Table 2. Spike detection results of the aforementioned improved and existing methods using the realistic synthetic neuronal data.

Method	TPS (mean ± SD)	FPS (mean ± SD)
Spike Detection based on AAPE and SSA	1 ± 0.00	0.03 ± 0.03
Spike Detection based on PE and SSA	0.99 ± 0.02	0.12 ± 0.08
AAPE-based approach	1 ± 0.00	0.25 ± 0.11
PE-based approach	0.99 ± 0.03	0.33 ± 0.14
Spike Detection based on FD and SSA [38]	1 ± 0.00	0.02 ± 0.03
NCED [45]	0.98 ± 0.04	0.23 ± 0.13

5.2. Real Data

5.2.1. Signal Segmentation Application

Signal segmentation is a required pre-processing stage for a number of biomedical signals such as EEG. Figure 6(a) depicts a real newborn EEG recording described in subsection 4.2.1. The window length and percentage of overlapping for two windows were chosen 700 samples (2.734 s) and 50%, respectively, and the embedding dimension was 5.

The results of applying the proposed method using PE and AAPE are shown in Figures 6 and 7, respectively. The real EEG signal is illustrated in Figure 6(a). Figures 6(b) and 6(c), respectively, illustrate the AAPE of the signal and changes in the G function. Using the EEG signal shown in Figure 6(a), we also employ the PE method for signal segmentation. Its result is depicted in Figure 7 (c). We also evaluate these methods on the other EEG signal depicted in Figures 8(a) and 9(a), in that order, for the AAPE and PE method. As can be seen in Figures 6 and 8, all the segments'

23

boundaries are accurately detected by AAPE, although for each signal, the method based on the PE incorrectly detects one boundary. Another significant difference between these results is that, in case of segments' boundaries, the changes of AAPE are larger than PE.

Using 40 real EEG signals, the performance of the proposed method using AAPE with DWT, PE with DWT, the approach based on DWT, KFD, and BCO [41], the method based on DWT, KFD, and PSO, AAPE, PE and WGLR are compared in Table 3. The best method in terms of both the TPS and FPS is the proposed approach based on AAPE and DWT, though not significantly different from signal segmentation based on DWT, KFD, and BCO. It is worth noting that the latter method (the propose approach) is considerably slower than the former one. The FD-based algorithms lead to better TPS and FPS ratios in comparison with the method using PE and DWT. Comparing the results obtained by the proposed and existing approaches with and without DWT shows the importance of the pre-processing step in signal segmentation. The SD values of the TPS and FPS ratios demonstrate that the proposed method based on AAPE with DWT is the most stable method among the proposed and existing EEG signal segmentation methods.
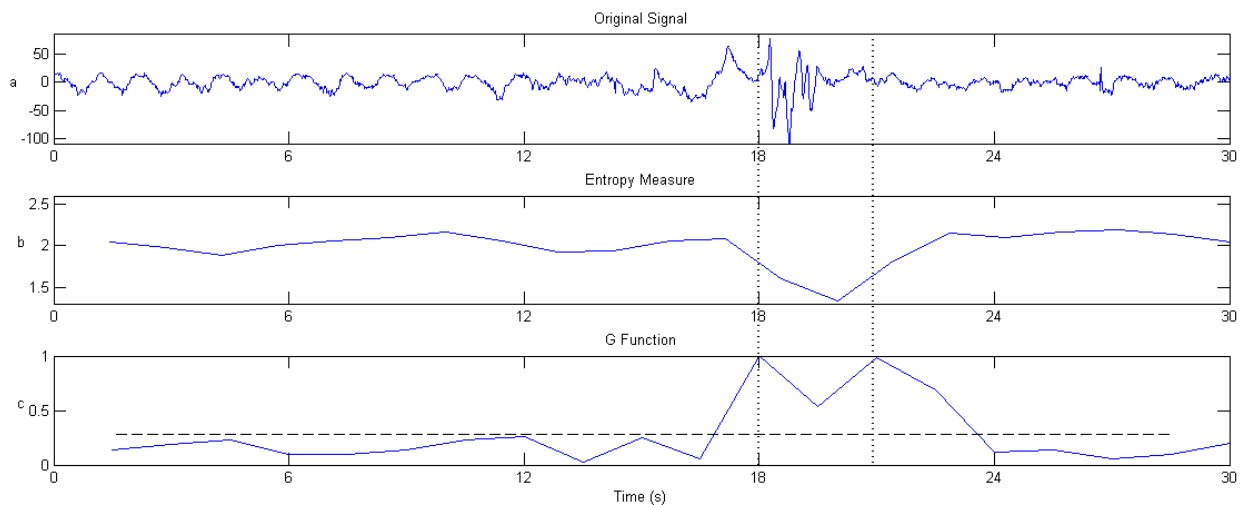
Figure 6. Result of the proposed technique for the real EEG signal; (a) original signal, (b) extracted features using the AAPE, and (c) *G* function result. The boundaries for all three segments are accurately detected.
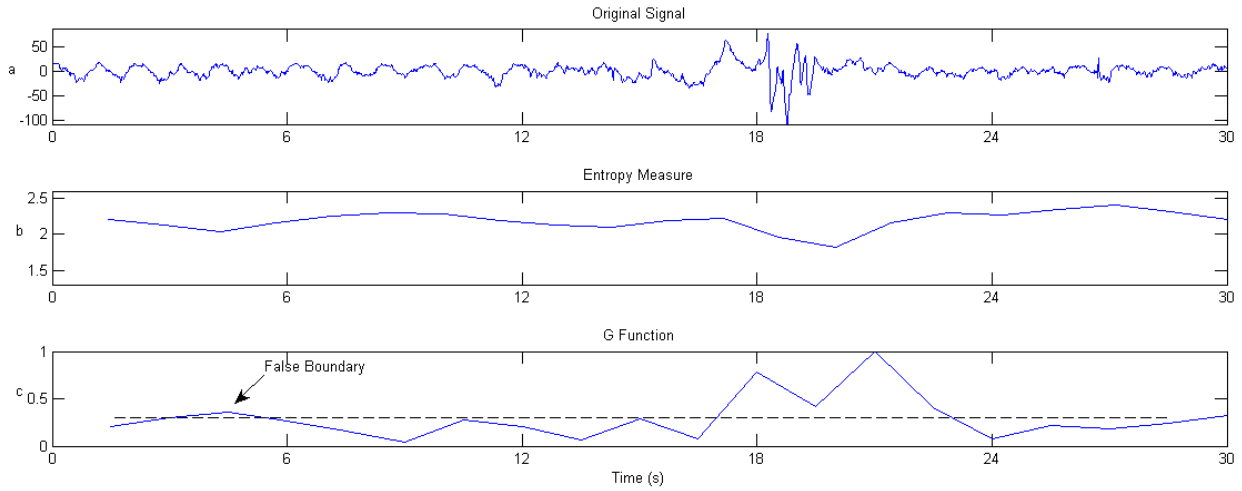

Figure 7. Result of the proposed technique for the real EEG signal; (a) original signal, (b) extracted features using the PE, and (c) *G* function result.

Figure 8. Result of the proposed technique for the real EEG signal; (a) original signal, (b) extracted features using the AAPE, and (c) *G* function result. The boundaries for all four segments are accurately detected.

Figure 9. Result of the proposed technique for the real EEG signal; (a) original signal, (b) extracted features using the PE, and (c) *G* function result.
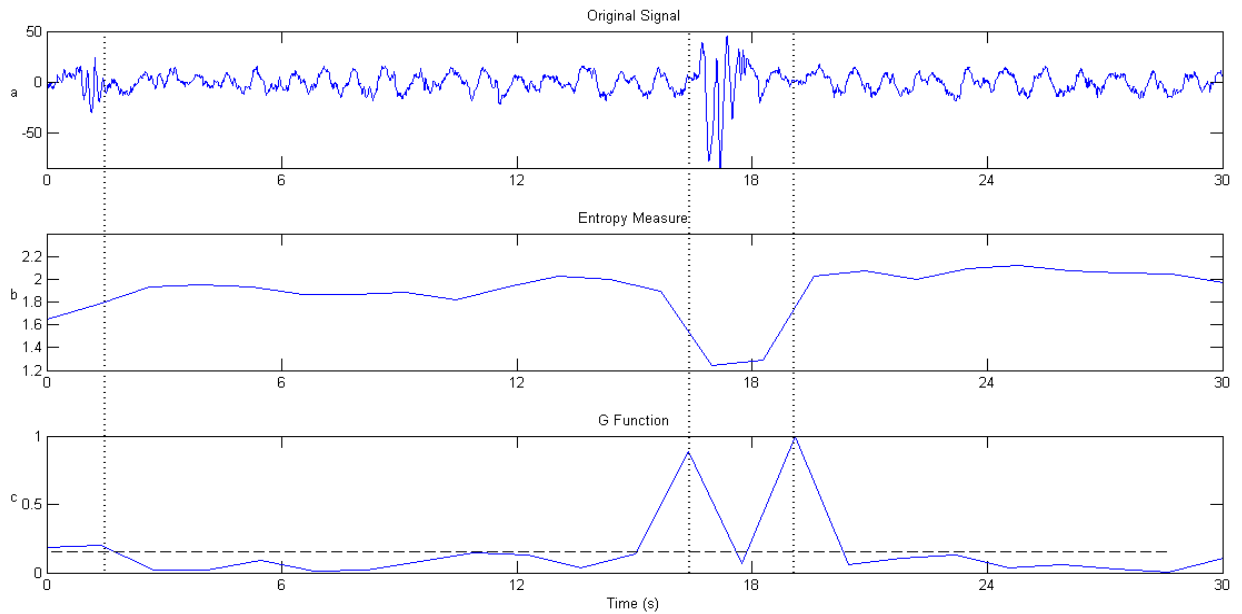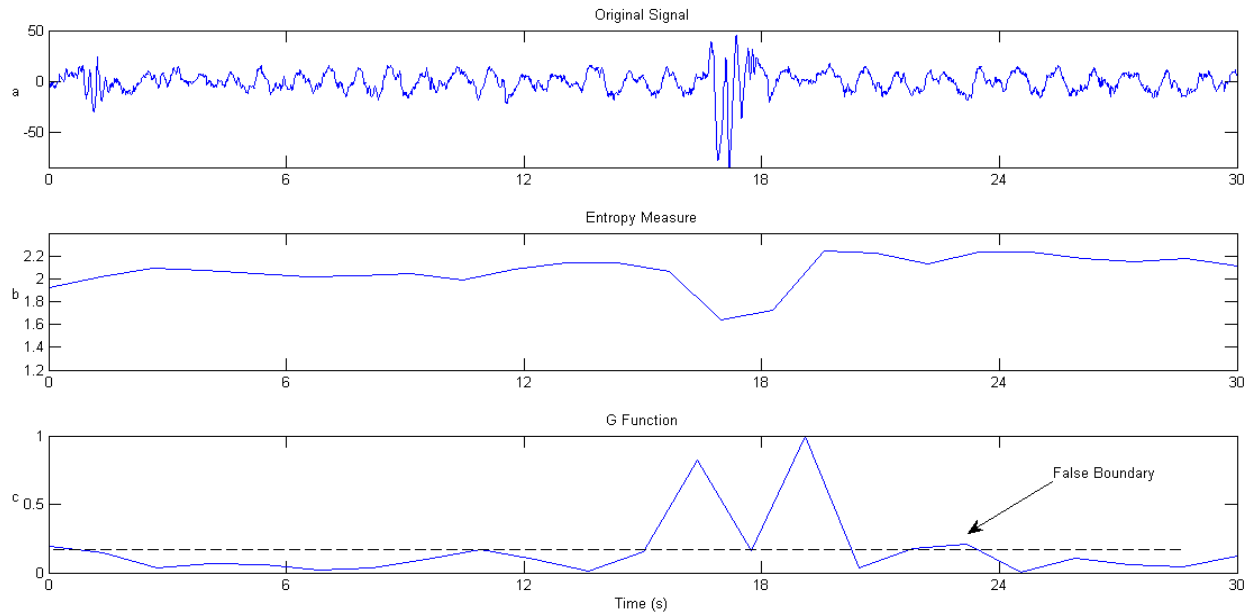
Table 3. Signal segmentation results of the aforementioned improved and existing methods using the EEG signals.

Method	TPS (mean ± SD)	FPS (mean ± SD)
Signal Segmentation based on DWT and AAPE	0.93 ± 0.13	0.08 ± 0.14
Signal Segmentation based on DWT and PE	0.84 ± 0.19	0.18 ± 0.21
Signal Segmentation based on DWT, KFD, and BCO [41]	0.89 ± 0.17	0.08 ± 0.16
Signal Segmentation based on DWT, KFD, and PCO [35]	0.87 ± 0.19	0.14 ± 0.19
AAPE-based approach	0.74 ± 0.17	0.16 ± 0.21

PE-based approach	0.73 ± 0.19	0.19 ± 0.19
WGLR [44]	0.69 ± 0.21	0.19 ± 0.22

5.2.2. Spike Detection Application

After evaluating the AAPE and PE methods on realistic synthetic neural data, in Figure 10, the performance of both of which are compared using the real neuronal data. This signal was described in subsection 4.2.2. As it can be observed, unlike the PE, the AAPE can detect the first spike. In Table 4, the results of using the above-mentioned spike detection approaches for real neuronal data explained in subsection 4.2.2 are demonstrated. The highest TPS ratios are achieved by the proposed method using AAPE and SSA. In terms of FPS, the best algorithms are the proposed method using the AAPE and FD and the method based on FD and SSA [38]. In terms of TPS and FPS parameters, both the AAPE and NCED have better performance than the PE. In terms of FPS the AAPE and NCED are alike, although in terms of TPS, the AAPE-based ratios are remarkably higher than the NCED method' ones. Note that because we studied on one real neuronal signal with about 200 spikes, the SD of TPS and FPS ratios are 0.
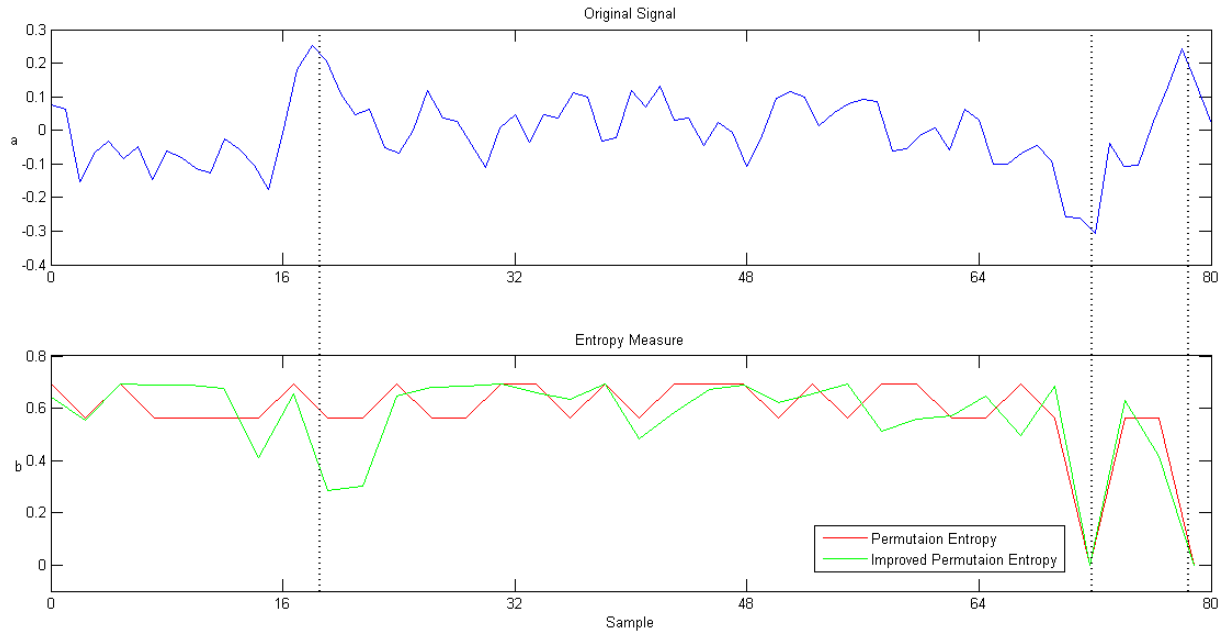
Figure 10. Results of applying AAPE and PE using real neuronal data. (a) Original signal, and (b) output of using PE and AAPE. All three spikes are be accurately detected by the use of AAPE although the PE does not change for the first spike.

Table 4. Spike detection results of the aforementioned improved and existing methods using the real neuronal data.

Method	TPS	FPS
Spike Detection based on AAPE and SSA	0.93	0.12
Spike Detection based on PE and SSA	0.90	0.21
AAPE-based approach	0.92	0.21
PE-based approach	0.88	0.28
Spike Detection based on FD and SSA [38]	0.91	0.12
NCED [45]	0.89	0.21

In future work, we will investigate the suitability of AAPE and multiscale AAPE to characterize other physiological time series, such as Alzheimer's disease.

5. Conclusions

PE is a powerful irregularity indicator, widely used for biomedical signal processing. However, since PE does not consider the mean value of amplitudes, differences between amplitude values and equal values, its use in some specific applications is limited. Accordingly, we have addressed these important shortcomings in this study. The proposed and existing algorithms have been applied in synthetic multi-component signals and EEG data for signal segmentation and realistic synthetic and real neuronal signals for spike detection application. Results have been compared with the original definition of PE and several other well-known approaches. For signal segmentation, the accuracy of AAPE-based approach has been superior to the accuracy of PE-based one as well as PE-based approaches have been more robust than WGLR in case of noise. In addition, the spike detection results have demonstrated when there is a single-sample spike, unlike PE, AAPE can detect spikes well. Moreover, for those spikes which include more than one sample point, the changes of AAPE values have been larger than those of PE values.

The weighted PE was proposed in [26] addresses the limitation of PE related to the fact that it disregards the information contained in the amplitude values. This method is only dependent on the variance, which measures the spread of the signal amplitudes, and its importance in the metric is always kept constant. In contrast, in AAPE, we can adapt the importance of mean values of amplitudes and differences between samples to different applications by means of *A*. Therefore, AAPE is more flexible. Unlike that method and PE, AAPE can also discriminate between an original signal and a constant number added to the original signal. As for the equal values' limitation, the algorithm proposed in [27] increases considerably the number of potential motifs. Hence, the algorithm might yield unreliable results for short signals. The algorithm proposed in [28] is sensitive to the precision regulation factor α. In contrast, AAPE does not have a sensitive

factor for this shortcoming. All in all, AAPE is a powerful tool to segment signals and detect spikes. It can be applied in different applications where the mean values of neighboring samples and changes in amplitude values are important. Our modification also deals with the equal amplitude values' problem. The AAPE's running time is slightly higher than the PE's one and it can be used in every entropy-based application.

Acknowledgments

Appendix

The AAPE Matlab code is available online at http://dx.doi.org/10.7488/ds/1339 .

References

[1]   A. Kowalski, M. Martín, A. Plastino, and O. Rosso, "Bandt–Pompe approach to the classical-quantum transition," *Physica D: Nonlinear Phenomena,* vol. 233, pp. 21-31, 2007.

[2]   S. Yin, X. Zhao, W. Wang, and M. Gong, "Efficient multilevel image segmentation through fuzzy entropy maximization and graph cut optimization," *Pattern Recognition,* vol. 47, pp. 2894-2907, 9// 2014.

[3]   L. Liu, B. Liu, H. Huang, and A. C. Bovik, "No-reference image quality assessment based on spatial and spectral entropies," *Signal Processing: Image Communication,* vol. 29, pp. 856-863, 9// 2014.

[4]   J. Wang, P. Shang, J. Xia, and W. Shi, "EMD based refined composite multiscale entropy analysis of complex signals," *Physica A: Statistical Mechanics and its Applications,* vol. 421, pp. 583-593, 3/1/ 2015.

[5]   M. Martínez-Zarzuela, C. Gómez, F. J. Díaz-Pernas, A. Fernández, and R. Hornero, "Cross-Approximate Entropy parallel computation on GPUs for biomedical signal analysis. Application to MEG recordings," *Computer Methods and Programs in Biomedicine,* vol. 112, pp. 189-199, 10// 2013.

[6]   S. Sanei, *Adaptive Processing of Brain Signals*: John Wiley & Sons, 2013.

[7]   S. M. Pincus, "Approximate entropy as a measure of system complexity," *Proceedings of the National Academy of Sciences,* vol. 88, pp. 2297-2301, 1991.

[8]   J. S. Richman and J. R. Moorman, "Physiological time-series analysis using approximate entropy and sample entropy," *American Journal of Physiology-Heart and Circulatory Physiology,* vol. 278, pp. H2039-H2049, 2000.

[9]   W. Chen, Z. Wang, H. Xie, and W. Yu, "Characterization of surface EMG signal based on fuzzy entropy," *Neural Systems and Rehabilitation Engineering, IEEE Transactions on,* vol. 15, pp. 266-272, 2007.

[10]   C. Bandt and B. Pompe, "Permutation Entropy: A Natural Complexity Measure for Time Series," *Physical Review Letters,* vol. 88, pp. 1-4, 2002.

[11]   O. A. Rosso, S. Blanco, J. Yordanova, V. Kolev, A. Figliola, M. Schürmann*, et al.*, "Wavelet entropy: a new tool for analysis of short duration brain electrical signals," *Journal of Neuroscience Methods,* vol. 105, pp. 65-75, 1/30/ 2001.

[12]   A. Holzinger, M. Hörtenhuber, C. Mayer, M. Bachler, S. Wassertheurer, A. Pinho*, et al.*, "On Entropy-Based Data Mining," in *Interactive Knowledge Discovery and Data Mining in Biomedical Informatics*. vol. 8401, A. Holzinger and I. Jurisica, Eds., ed: Springer Berlin Heidelberg, 2014, pp. 209-226.

[13]   K. Keller, A. M. Unakafov, and V. A. Unakafova, "Ordinal Patterns, Entropy, and EEG," *Entropy,* vol. 16, pp. 6212-6239, 2014.

[14]   M. Zanin, L. Zunino, O. A. Rosso, and D. Papo, "Permutation Entropy and Its Main Biomedical and Econophysics Applications: A Review," *Entropy,* vol. 14, pp. 1553-1577, 2012.

[15]   Y.-J. Yuan, X. Wang, Z.-T. Huang, and Z.-C. Sha, "Detection of Radio Transient Signal Based on Permutation Entropy and GLRT," *Wireless Personal Communications,* pp. 1-11, 2015/01/07 2015.

[16]   G. Zhu, Y. Li, P. Wen, and S. Wang, "Classifying Epileptic EEG Signals with Delay Permutation Entropy and Multi-scale K-Means," in *Signal and Image Analysis for Biomedical and Life Sciences*. vol. 823, C. Sun, T. Bednarz, T. D. Pham, P. Vallotton, and D. Wang, Eds., ed: Springer International Publishing, 2015, pp. 143-157.

[17]   J. M. Amigó, L. Kocarev, and J. Szczepanski, "Order patterns and chaos," *Physics Letters A,* vol. 355, pp. 27-31, 2006.

[18]   M. Matilla-García and M. R. Marín, "A non-parametric independence test using permutation entropy," *Journal of Econometrics,* vol. 144, pp. 139-155, 2008.

[19]   L. Zunino, A. F. Bariviera, M. B. Guercio, L. B. Martinez, and O. A. Rosso, "On the efficiency of sovereign bond markets," *Physica A: Statistical Mechanics and its Applications,* vol. 391, pp. 4342-4349, 2012.

[20]   H. Azami and J. Escudero, "Improved multiscale permutation entropy for biomedical signal analysis: Interpretation and application to electroencephalogram recordings," *Biomedical Signal Processing and Control,* vol. 23, pp. 28-41, 1// 2016.

[21]   J. Li, J. Yan, X. Liu, and G. Ouyang, "Using Permutation Entropy to Measure the Changes in EEG Signals During Absence Seizures," *Entropy,* vol. 16, pp. 3049-3061, 2014.

[22]   H. Azami, K. Smith, A. Fernandez, and J. Escudero, "Evaluation of resting-state magnetoencephalogram complexity in Alzheimer's disease with multivariate multiscale permutation and sample entropies," in *Engineering in Medicine and Biology Society (EMBC), 2015 37th Annual International Conference of the IEEE*, 2015, pp. 7422-7425.

[23]   G. Ouyang, C. Dang, D. A. Richards, and X. Li, "Ordinal pattern based similarity analysis for EEG recordings," *Clinical Neurophysiology,* vol. 121, pp. 694-703, 2010.

[24]   E. Olofsen, J. Sleigh, and A. Dahan, "Permutation entropy of the electroencephalogram: a measure of anaesthetic drug effect," *British journal of anaesthesia,* vol. 101, pp. 810-821, 2008.

[25]   S. Schinkel, N. Marwan, and J. Kurths, "Brain signal analysis based on recurrences," *Journal of Physiology-Paris,* vol. 103, pp. 315-323, 2009.

[26]   B. Fadlallah, B. Chen, A. Keil, and J. Príncipe, "Weighted-permutation entropy: A complexity measure for time series incorporating amplitude information," *Physical Review E,* vol. 87, p. 022911, 02/20/ 2013.

[27]   C. Bian, C. Qin, Q. D. Y. Ma, and Q. Shen, "Modified permutation-entropy analysis of heartbeat dynamics," *Physical Review E,* vol. 85, p. 021906, 02/10/ 2012.

[28]   L. Xiao-Feng and W. Yue, "Fine-grained permutation entropy as a measure of natural complexity for time series," *Chinese Physics B,* vol. 18, p. 2690, 2009.

[29]   S. Sanei and J. Chambers, *EEG signal processing*: John Wiley & Sons, 2008.

[30]   H. Azami, S. Sanei, K. Mohammadi, and H. Hassanpour, "A hybrid evolutionary approach to segmentation of non-stationary signals," *Digital Signal Processing,* vol. 23, pp. 1103-1114, 7// 2013.

[31]   H. Azami, H. Hassanpour, and S. Anisheh, "An Improved Automatic EEG Signal Segmentation Method based on Generalized Likelihood Ratio," *International Journal of Engineering-Transactions A: Basics,* vol. 27, p. 1015, 2014.

[32]   R. Zimroz, M. Madziarz, G. Żak, A. Wyłomańska, and J. Obuchowski, "Seismic signal segmentation procedure using time-frequency decomposition and statistical modelling," 2015.

[33]   R. Agarwal and J. Gotman, "Adaptive segmentation of electroencephalographic data using a nonlinear energy operator," in *Circuits and Systems, 1999. ISCAS '99. Proceedings of the 1999 IEEE International Symposium on*, 1999, pp. 199-202 vol.4.

[34]   S. Mahmoodi and B. S. Sharif, "Signal segmentation and denoising algorithm based on energy optimisation," *Signal Processing,* vol. 85, pp. 1845-1851, 9// 2005.

[35]   S. Anisheh and H. Hassanpour, "Designing an adaptive approach for segmenting non-stationary signals," *International Journal of Electronics,* vol. 98, pp. 1091-1102, 2011.

[36]   H. Azami, J. Escudero, A. Darzi, and S. Sanei, "Extracellular spike detection from multiple electrode array using novel intelligent filter and ensemble fuzzy decision making," *Journal of Neuroscience Methods,* vol. 239, pp. 129-138, 1/15/ 2015.

[37]   J. Martinez, C. Pedreira, M. J. Ison, and R. Quian Quiroga, "Realistic simulation of extracellular recordings," *Journal of Neuroscience Methods,* vol. 184, pp. 285-293, 11/15/ 2009.

[38]   H. Azami and S. Sanei, "Spike detection approaches for noisy neuronal data: Assessment and comparison," *Neurocomputing,* vol. 133, pp. 491-506, 6/10/ 2014.

[39]   M. Costa, A. L. Goldberger, and C.-K. Peng, "Multiscale Entropy Analysis of Complex Physiologic Time Series," *Physical Review Letters,* vol. 89, pp. 1-4, 2002.

[40]   L. S. Smith and N. Mtetwa, "A tool for synthesizing spike trains with realistic interference," *Journal of Neuroscience Methods,* vol. 159, pp. 170-180, 1/15/ 2007.

[41]   H. Azami, H. Hassanpour, J. Escudero, and S. Sanei, "An intelligent approach for variable size segmentation of non-stationary signals," *Journal of Advanced Research,* 2014.

[42]   M. E. Kirlangic, D. Perez, S. Kudryavtseva, G. Griessbach, G. Henning, and G. Ivanova, "Fractal dimension as a feature for adaptive electroencephalogram segmentation in epilepsy," in *Engineering in Medicine and Biology Society, 2001. Proceedings of the 23rd Annual International Conference of the IEEE*, 2001, pp. 1573-1576 vol.2.

[43]   R. Esteller, G. Vachtsevanos, J. Echauz, and B. Litt, "A comparison of waveform fractal dimension algorithms," *Circuits and Systems I: Fundamental Theory and Applications, IEEE Transactions on,* vol. 48, pp. 177-183, 2001.

[44]   L. Jun, L. Xing, and L. Tong, "Web-Based Application for Traffic Anomaly Detection Algorithm," in *Internet and Web Applications and Services, 2007. ICIW '07. Second International Conference on*, 2007, pp. 44-44.

[45]   N. Mtetwa and L. S. Smith, "Smoothing and thresholding in neuronal spike detection," *Neurocomputing,* vol. 69, pp. 1366-1370, 6// 2006.